

however, no assignment seems to be available for resonance (12).

³⁵P. C. von Planta, *J. Opt. Soc. Am.* **47**, 629 (1957).

³⁶This program is available in the Share Distribution Library (Share Distribution No. 1428.)

For an outline of the method see also D. W. Marquardt, *J. Soc. Ind. Appl. Math.* **11**, 431 (1963).

³⁷F. J. Comes and H. G. Sälzer, *Phys. Rev.* **152**, 29 (1966).

³⁸The authors of Ref. 21 have since withdrawn this suggested form of the dependence of Γ on n^* . Their discussion of this matter is contained in Ref. 40.

³⁹The fraction of the underlying continua with which the discrete level can interact while still preserving the oscillator strength concept depends on the q of the resonance. The higher the q , the larger the fraction of the continua with which interaction can be tolerated.

⁴⁰U. Fano and J. W. Cooper, *Rev. Mod. Phys.* **40**, 441 (1968).

⁴¹F. H. Mies, *Phys. Rev.* **175**, 164 (1968).

⁴²In Fig. 3, the $3s\ 3p^6\ np\ ^1P_1^\circ$ series merges because of the finite width of the slit at about the level $n=20$. Above this point the slit transmits the intensity averaged over several resonances. The change in transmission registered by the detector at this point is a good approximation to the change in transmission that is observed beyond the series limit. This is not true for a series of sharp (compared to the slit) absorption resonances, where the transmission averaged over several resonances is a gross underestimate of the continuum transmission.

⁴³R. W. Alexander, D. L. Ederer, and D. H. Tomboulian, *Bull. Am. Phys. Soc.* **9**, 626 (1964).

⁴⁴J. W. Cooper, *Phys. Rev.* **128**, 681 (1962).

⁴⁵M. Conneely, L. Lipsky, and K. Smith in *Fifth International Conference on the Physics of Electronic and Atomic Collisions* edited by I. P. Flaks and E. S. Solovoyov (Nauka, Leningrad, 1967), p. 619.

⁴⁶P. G. Burke and K. Smith, *Rev. Mod. Phys.* **34**, 458 (1962).

Photo-Ionization of Krypton Between 300 and 1500 eV. Relative Subshell Cross Sections and Angular Distributions of Photoelectrons*

Manfred O. Krause

Oak Ridge National Laboratory, Oak Ridge, Tennessee 37830

(Received 18 July 1968)

Energy spectra of electrons ejected from M and N subshells of krypton by characteristic x rays of 300 to 1500 eV energy have been measured with an electrostatic analyzer. Krypton was irradiated in the gas phase and electrons were detected perpendicular to the x-ray beam. From these spectra, relative subshell contributions to the photo-ionization cross section were obtained for single-electron emission and for double-electron emission, the latter involving simultaneous transitions of M and N electrons. Angular distributions of photoelectrons from $3s$, $3p$ and $3d$ shells of krypton and $1s$ shell of neon also have been determined at excitation energies from about 200 to 1100 eV above the respective ionization thresholds. Data on relative cross sections for single photo-ionization corroborate a theoretical model which uses a Herman-Skillman central potential (Cooper and Manson in the following article). Angular distributions agree satisfactorily with calculations by the same model; this means theory makes dependable predictions regarding the asymmetry parameter and the effect of retardation. Data on double photo-ionization disagree with results of the electron shakeoff theory which accounts for only about half the observed intensities. This suggests that electron-electron correlation plays an important role.

I. INTRODUCTION

Since the conception of the hydrogenic model of photo-ionization it has been known that this model would become increasingly inadequate with decreasing photon energy and increasing quantum number of the electrons.¹ Recent experimental studies²⁻⁵ of total photoabsorption cross sections of rare gas atoms have shown its complete failure in the soft x-ray region. On the theoretical side⁶ great improvements were achieved by using a more realistic central field than given in the hydrogenic approximation. Aside from causing the familiar sharp absorption edges to disappear, the

new treatment^{7,8} of photo-ionization resulted in irregular patterns of the individual subshell cross sections, both in magnitude and energy dependence, in contrast to the predictions of the hydrogenic model.⁹ It is this behavior that makes measurements of subshell cross sections desirable, even on a relative basis, thus providing a direct test of specific results of theory. In the present study this was done by measuring the energy spectra of photoelectrons escaping from M and N subshells of krypton. Observation of photoelectrons from free atoms excluded complications arising from solid state or chemical effects and singled out photo-ionization events proper from other proces-

ses that enter in most of the conventional determinations of photo-ionization cross sections. As a further advantage of the present method, single-electron transitions could be distinguished from double (multiple)-electron transitions in a manner described previously.^{10,11}

Relative subshell cross sections for single and double photo-ionization were obtained at right angles to the x-ray beam in the energy range from 300 to 1500 eV. Data for single-electron emission give strong support to a theoretical model which is based on a realistic central potential of the atom; experiment and theory are compared in the companion article by Cooper and Manson.¹² Data on double photo-ionization, involving an *MN* pair of electrons, are compared in Sec. III. B with results of the electron shake-off theory which was employed earlier to interpret observations on *KL* photo-ionization of neon and argon and *KM* ionization of argon.¹⁰

Another important facet of photo-ionization is the angular distribution of the escaping electron. Besides being a requisite for conversion of (measured) differential cross sections into total cross sections the measurement of the directional dependence of photoelectron emission subjects theory to further sensitive tests: 1) It determines the parameters *A* and *B* of the angular distribution function $J(\theta) = A + B \sin^2\theta$ or, alternatively, the asymmetry parameter $\beta = 4B/(3A + 2B)$ whose dependence on atomic quantities is given by Eq. (11) of Ref. 12; and 2) it determines the effect of retardation. It is worthwhile to mention that the parameter β has not been measured or calculated previously except for some early qualitative estimates¹³ and some recent measurements by Berkowitz *et al.*¹⁴ at an isolated photon energy of 21 eV. Retardation, however, was the subject of many investigations^{1,13,15} in the hard x-ray region where its effect is greatest, but investigations in the soft x-ray region have not been undertaken. In this paper angular distributions are reported for photoelectrons from 3*s*, 3*p* and 3*d* subshells of krypton and from 1*s* shell of neon at relatively low photoelectron energies of 200 to 1100 eV. The present experiment combines advantages of previously used methods, namely, gaseous target¹⁶ and differential energy analysis.^{15,17} Results are presented in Secs. III. C and D, whereas theoretical details of this aspect of photo-ionization are given in Ref. 12.

II. EXPERIMENTAL

A sketch of the apparatus is shown in Fig. 1. The device differs from the previously described instrument¹⁸ in the addition of a rotatable source chamber, an improved compensation of stray magnetic fields and the use of a new miniature x-ray tube with exchangeable target. X rays were collimated to a narrow beam of small divergence, $\alpha \lesssim 1^\circ$, and electrons emitted into a cone with apex angle of 2° about the electron-optical axis were analyzed and detected individually by a DuMond SP174 electron multiplier. *K* and *L* lines from various anodes were utilized; a polystyrene filter of $20 \mu\text{g}/\text{cm}^2$ for radiation below

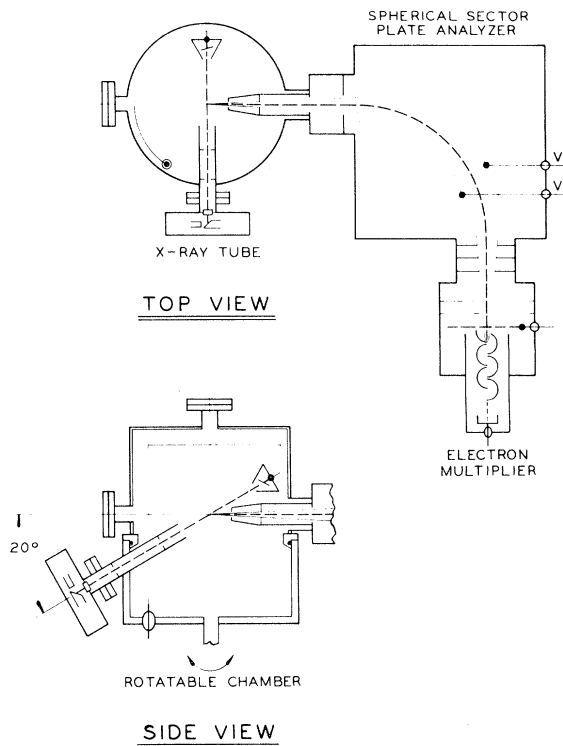


FIG. 1. Schematic of apparatus. Turret chamber allows continuous variation of angle between x-ray and electron-optical axis from 20° to 145° and from -20° to -90° .

600 eV and of $65 \mu\text{g}/\text{cm}^2$ above 600 eV separated the x-ray tube from the gas cell. Gas pressures were in the order of 10^{-2} Torr in the source, less than 2×10^{-5} Torr in the analyzer and less than 1×10^{-6} Torr in the x-ray tube. The angle between directions of photons and observed electrons could be varied continuously from 20° to 145° and from -20° to -90° . The x-ray tube could be rotated about the collimator axis to explore possible presence of any polarization of the photons.

Electron spectra were recorded by applying a repetitive dc biased sawtooth voltage to the analyzer plates and storing the signals in the memory core of a multiscaler synchronized with the sawtooth. Ordinarily, each scan comprised the entire energy range in which photoelectrons produced by a given x-ray line should appear. For most of the runs the resolution of the instrument was set to $\Delta E/E = 1.5\%$ (full width at half-maximum), and in some cases an improved resolution of 0.9% was used. All measurements of electron spectra were performed at an angle of 90° between photon and electron propagation directions. In each experiment an excellent signal-to-background ratio was achieved due to the low noise level of the detector, about 0.4 counts/min, and the strengths of the characteristic x-ray lines above the underlying bremsstrahlung continuum.

For angular measurement voltages of the analyzer were set to the peak of the photoline under in-

vestigation and the position of the x-ray tube was changed in steps. Angular resolution was (4 ± 0.7) deg, as given by the divergence of both x-ray and electron beam. Measured intensities were multiplied by $f \sin\theta$ to normalize to constant source volume. The factor f increased from 1.00 at $\theta = \pm 90^\circ$ to 1.07 ± 0.03 at $\theta = 20^\circ$ (160°) and was determined from auxiliary runs on the Ne 1s-2p2p Auger line which has a spherically symmetrical intensity distribution. It accounts for a combination of errors introduced by the possible inhomogeneity of the finite source, inelastic scattering losses, and possible deviation of the actual angle from the indicated angle. Gas pressure proved to be sufficiently steady with fluctuations of less than 2%, and x-ray flux was controlled manually by reference to the reading of a Faraday-cup monitoring device. A potential change in the intensity of the characteristic x-ray lines was checked by referring periodically to the photoelectron count rate at $\theta = 90^\circ$. To insure against distortions from elastic scattering a number of runs were made at different pressures, and to verify the symmetry of the arrangement as well as insensitivity to the magnetic field of the filament current of the x-ray tube, data were also taken at negative angles. Errors from sources outlined above were small except for short-term instabilities of the x-ray tube output. Statistical confidence of $\pm 5\%$ could be achieved in relatively short times as peak counting rates were 100 to 400 counts/min for the more intense photolines, i. e., those corresponding to the emission of a Kr 3d or a Ne 1s electron.

III. RESULTS

A. Relative Subshell Cross Sections for Single-Electron Transitions at $\theta = 90^\circ$

Figure 2 shows the photoelectron spectrum $KrM(CuL)$ observed perpendicular to the x-ray beam. An average background of 12 counts per channel has been subtracted, thus accounting for detector noise, about 4 counts, and contributions from bremsstrahlung, about 8 counts. The spectrum shows that relative intensities of photoelectron emission from various subshells can be obtained with ease at a moderate energy resolution and without the necessity of using a monochromatic x-ray source. The possibility of subtracting the bremsstrahlung contribution, which can be evaluated from regions where no lines appear, allows us to remove automatically any discrimination that may be caused by polarization of this type of quanta. The spectrum displayed shows, however, one of the rare cases when two different photolines coincide, namely the $KrM_3(CuL_\alpha)$ and $KrM_{4,5}(CuL_1)$ lines. (Atomic energy levels are denoted here by subscripts in arabic numerals.) To be able to correct for the presence of the $KrM_{4,5}(CuL_1)$ line, relative intensities of the CuL x rays were determined from the $ArL(CuL)$ photoelectron spectrum in a separate experiment.

Cross sections at $\theta = 90^\circ$ of 3s, 3p, 4s, and 4p subshells relative to the 3d cross section are

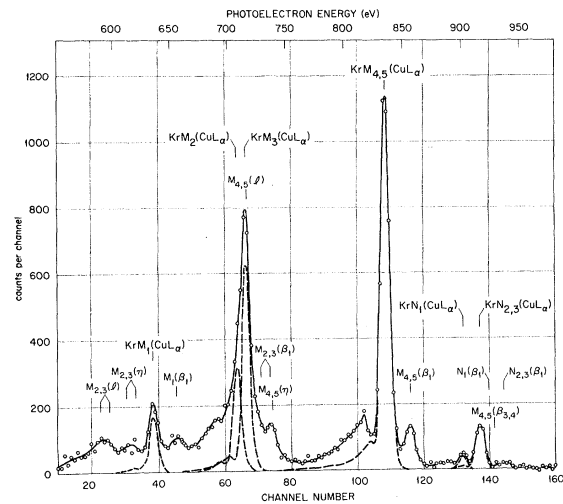


FIG. 2. Electron spectrum $KrM(CuL)$ and $KrN(CuL)$, observed at right angles to x-ray beam with $\Delta E/E = 0.9\%$. Lines due to CuL_α line have been resolved graphically (dash lines). Abbreviated symbols, i. e., $M_{4,5}(l) \hat{=} KrM_{4,5}(CuL_l)$, indicate weaker photolines; some faint lines have not been denoted in the graph. Note that another spectrum, $KrM(MgK_\alpha)$, is shown in Fig. 3(a).

tabulated in Table I for 11 x-ray lines ranging from $CK_\alpha = 277$ eV to $AlK_\alpha = 1487$ eV. Intensities are area values averaged from up to 4 determinations per excitation energy and are corrected for dispersion of analyzer, background, overlapping photo- and Auger lines, continuum of two-electron transitions and variation of detection efficiency with energy. Quoted errors are weighted averages of the errors for the individual runs which, in turn, reflect uncertainties in statistics and the required corrections. M - NN Auger lines were disturbing at energies below 170 eV, and L - MM lines disturbed above 1200 eV. This interference is responsible for the large errors of the intensities for $KrM_{2,3}(CK_\alpha)$ and $KrM(AlK_\alpha)$ and the omission of values for the weak $KrN(MgK_\alpha)$ and $KrN(AlK_\alpha)$ lines which were obliterated by strong Auger lines. Errors have not been assigned to 4s and 4p contributions, but only to their sums, if the lines were poorly resolved or when the statistical uncertainty was large.

As seen from Table I the relative probability of ejecting an electron from the 3d level remains high over the entire range investigated whereas the probability of electron emission for the 3s level remains low. Photo-ionization in the 3p shell becomes more significant with increasing photon energy. Predominance of the 3d contribution would be accentuated if we were to transpose these cross sections measured at 90° to total subshell cross sections by utilizing angular electron distributions given in Sec. III.C. This behavior of the subshell contribution could have been suspected qualitatively from the trend of the total photoabsorption cross sections² and from measurements of final charge states following inner-shell photo-ionization.¹⁹ The hydrogenic model of photo-

TABLE I. Subshell contributions to photo-ionization cross section of krypton at $\theta = 90^\circ$. Values are in percent relative to cross section of $3d$ subshell.

| Photon line | Photon energy (eV) | Shell | | | | |
|--------------|--------------------|----------------|----------------|---------------|---------------|----------------|
| | | 3s | 3p | 4s | 4p | N |
| CK_α | 277 | 0 | 33 ± 12 | 2.5 | 4 | 6.5 ± 2.5 |
| TiL_α | 452 | 15 ± 6 | 48 ± 8 | 3.5 ± 1.2 | 6.0 ± 1.5 | 9.5 ± 1.5 |
| CrL_l | 500 | 21 ± 5 | 44 ± 10 | ... | ... | ... |
| OK_α | 525 | 14 ± 2 | 51 ± 3 | 2.8 ± 0.4 | 5.2 ± 0.5 | 8.0 ± 0.7 |
| CrL_α | 573 | ... | 49 ± 8 | 3.5 | 5.5 | 9 ± 2 |
| FeL_α | 705 | 17 ± 7 | 75 ± 10 | 7 | 15 | 22 ± 7 |
| NiL_α | 852 | 15 ± 5 | 89 ± 8 | 6 | 10 | 16 ± 4 |
| CuL_α | 930 | 20.8 ± 1.5 | 95.5 ± 2.5 | 3.8 ± 0.6 | 9.7 ± 0.8 | 13.5 ± 1.0 |
| ZnL_α | 1012 | 20 ± 3 | 106 ± 6 | 7 | 9 | 16 ± 2 |
| MgK_α | 1254 | 35 ± 3 | 128 ± 6 | ... | ... | ... |
| AlK_α | 1487 | 50 ± 15 | 160 ± 15 | ... | ... | ... |

ionization is in gross disaccord with experiment as it yields, for example, a cross section ratio σ_{3p}/σ_{3d} too great by a factor of about 10 over the reported energy range, but a theory in which a realistic central potential¹² (i.e., Herman-Skillman's) is used gives good agreement with experimental findings.

B. Relative Intensities of Double-Electron Transitions.

In Sec. III.A, I refer only to the discrete peaks of the electron spectra, thereby selecting events in which one photon ejects a single electron. If we examine the continuum distributions on the low-energy side of each photoline seen in Figs. 2 and 3(a) we find, in analogy to earlier studies,^{10,11} that they give evidence of processes in which a single photon causes multiple, especially double, electron transitions.²⁰ Briefly, these continua arise from the fact that the remainder of the photon energy, which is left after "prying loose" a second electron, is shared among two electrons in such a way, that one electron takes up a small amount of energy and the other electron takes up a correspondingly large amount, and thus appears near the photoline of the single photo-ionization process.

The following intensities of multiple-electron transitions per ionization event are deduced from the areas of the continua and their parent photo-peaks after some minor corrections¹⁰ have been made: $(23 \pm 2)\%$ for $3dN$ electrons, about 22% for both $3pN$ and NN electrons, and roughly 18% for $3sN$ electrons. Except for NN electrons these values refer to excitation by MgK_α x rays, but similar values were obtained for excitation by softer radiation, such as CuL_α and OK_α x rays. Multiple ionization makes, therefore, a substantial contribution to the photo-ionization cross section. Though the phenomenon is not recognized in the single-electron model²¹ it may be treated with the aid of the electron-shakeoff concept as a two-stage process each involving one electron: first, photo-ionization proper with the emission of the first electron, second, ionization of a second electron as a result of the sudden change in screening

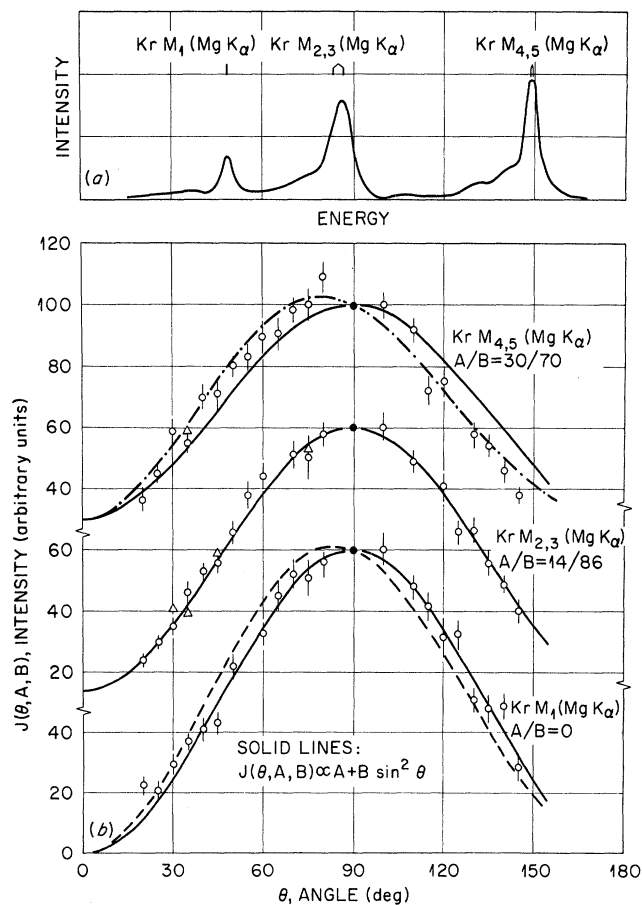


FIG. 3. (a) Recording of $KrM(MgK_\alpha)$ electron spectrum. (b) Angular distributions of $3s$, $3p$ and $3d$ photo-electrons ejected by MgK_α x rays. Angular resolution (4 ± 0.7) deg, and $J(90^\circ) = 100$. Triangles represent measurements at negative angles and have about the same error bars as points at positive angles. Dashed line according to $J(\theta) = [1 + 4(v/c) \cos \theta] \sin^2 \theta$; and dash-dotted line according to evaluation of Ref. 12: $J(\theta) = 0.3 + 0.7[1 + 6(v/c) \cos \theta] \sin^2 \theta$.

when the first electron has escaped the atom. This procedure has proven successful in the case of *KL* photo-ionization¹⁰ of Ne and Ar, but it has failed in the case of double ionization in the outer shells¹¹ of He, Ne, and Ar. On the same basis a probability of about 12% was calculated^{19,22} for losing and *N* electron of Kr together with any of the *M* electrons. This approach accounts for only half the observed intensity, indicating that electron-electron correlation between *M* and *N* electrons and among *N* electrons of Kr might be similarly significant as it was found to be for the electrons in He. There, inclusion of correlation between the electrons in the ground state gave good agreement with the experiment.²³

C. Angular Distribution of Photoelectrons from *M* Subshells of Krypton.

Angular distributions of 3*s*, 3*p* and 3*d* electrons excited by MgK_α x rays are shown in Fig. 3(b). Data points are averaged from three runs and error bars indicate the uncertainties mainly due to statistical and x-ray flux fluctuations. A small correction was applied to the KrM_{2,3}(MgK_α) distributions and a somewhat larger one to the KrM₁(MgK_α) distribution to eliminate distortions from the double-ionization continua, the angular distributions of which were found to be approximately the same as those for the respective parent lines. As pointed out in Sec. III.A weakly polarized bremsstrahlung quanta had negligible effect also on the angular distributions (with the setup of Fig. 1 the polarization sensitive azimuthal angle is also changed). Solid lines in Fig. 3(b) correspond to the relation $J(\theta) = A + B \sin^2\theta$ with the parameters *A* and *B* chosen to give a best fit. The angular dependence for 3*s* electrons exhibits no isotropic part in accordance with theory,¹ while the isotropic contribution for 3*p* and 3*d* electrons is in good agreement with the calculation of Cooper and Manson.¹² The effect of retardation leading to a preferential electron ejection into the forward direction, $\theta < 90^\circ$, is markedly different for the various subshell electrons, although their velocities are nearly the same. The 3*d* distribution fits rather well the dash-dotted curve corresponding to

$$J(\theta) = 0.3 + 0.7[1 + 6(v/c) \cos\theta] \sin^2\theta,$$

where the term in brackets gives the retardation correction;¹² the 3*p* and 3*s* distributions show, however, no significant shift due to retardation. This is in agreement with an evaluation given in Ref. 12, but note the poor agreement with this experiment of the relation

$$J(\theta) = [1 + 4(v/c) \cos\theta] \sin^2\theta$$

derived earlier.^{1,9} At lower excitation energies the 3*s* and 3*p* angular intensities retain their symmetry and the 3*d* distribution becomes less and less asymmetric.

Table II compiles experimental determinations of the parameters *A* and *B* measured for a number of excitation energies. Quoted errors allow

for the possibility of drawing different curves through the experimental points and, in some cases for the uncertainty in the correction for the double-ionization continuum which extended into the region of the photoline. Experimental data for the parameters *A* and *B* are satisfactorily accounted for by the theoretical calculations of Ref. 12.

D. Angular Distribution of Photoelectrons from 1*s* Shell of Neon

I present these data in conjunction with the results on krypton since angular distributions of *s* photoelectrons have not been measured at small energies, that is below a few keV, and since distributions of 3*s* electrons of krypton were somewhat uncertain because of the weakness of the photolines and the relatively large "background" correction. In the case of neon the photolines are, however, very strong and the background correction amounts to barely 1% of the counts at $\theta = 90^\circ$. The distributions shown in Fig. 4 for three photoelectron energies should lie in the range of validity of the relation^{1,12}

$$J(\theta) = [1 + 4(v/c) \cos\theta] \sin^2\theta.$$

As seen from the figure, the theoretical shape fits the experimental data satisfactorily, although there seems to be a tendency for the experimental distribution to be slightly less shifted than indicated by the above relation.

IV. FINAL REMARKS

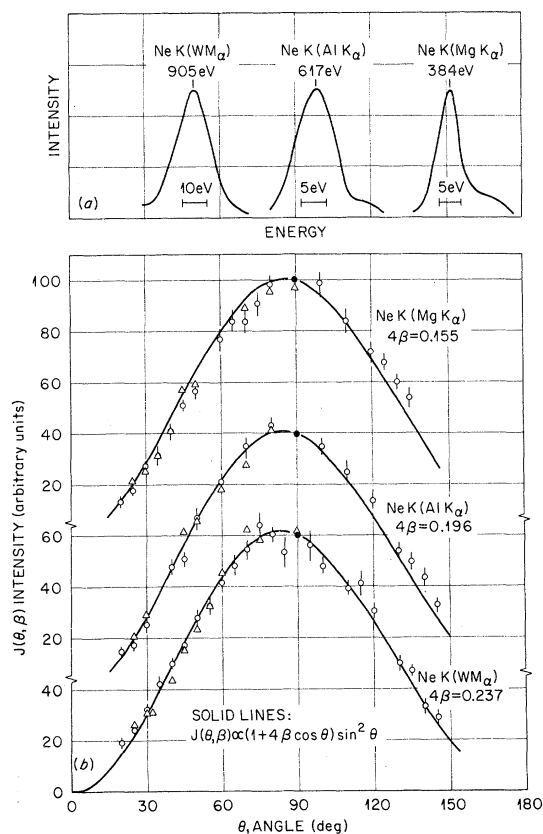
In this study the potential of electron spectrometry was utilized to determine subshell contributions to the photo-ionization cross section.²⁴ Such data are essential to theory, especially in the soft x-ray region where cross sections are very sensitive to the wave functions and approximations that are incorporated in a particular model. Substantial agreement of the present data on krypton with calculations¹² based on a realistic central-field model suggests that this model will also be trustworthy in other cases²⁵ as far as single-electron contributions are concerned. The agreement implies further that two-electron processes observed in this experiment affect the energy dependence of single-electron emission from the various subshells either in the same way or not at all. At the present time, only relative cross sections were obtained, but determination of absolute cross sections is feasible. This would be useful for investigations near ionization thresholds and also at higher energies, where scattering events and multiple ionization processes are more difficult to appraise.

Measurements of electron energy spectra yield information on multiple-electron excitation in the photoabsorption process. This phenomenon, which accompanies single-electron excitation in typically 20% of the photo-ionization events, has not yet been treated in a unified general manner.²⁶

Finally, theoretical predictions of the asymmetry parameter β and the retardation term can be tested by measuring angular distributions of pho-

TABLE II. Parameters A and B of angular distribution $J(\theta) = A + B \sin^2 \theta$ of photoelectrons ejected from M subshells of krypton by soft x rays. $A + B = 100$.

| Shell | Photon line | Photon energy (eV) | Photoelectron energy (eV) | A | B | $\sigma \pm$ of A and B |
|-------|-----------------|--------------------|---------------------------|------|------|-----------------------------|
| 3d | CK $_{\alpha}$ | 277 | 182 | 47 | 53 | 5 |
| | TiL $_{\beta}$ | 395 | 300 | 33 | 67 | 3 |
| | TiL $_{\alpha}$ | 452 | 357 | 35 | 65 | 3 |
| | OK $_{\alpha}$ | 525 | 430 | 35 | 65 | 2 |
| | CuL $_{\alpha}$ | 930 | 835 | 35 | 65 | 3 |
| | MgK $_{\alpha}$ | 1254 | 1159 | 30 | 70 | 4 |
| 3p | TiL $_{\alpha}$ | 452 | 235 | 10 | 90 | 5 |
| | OK $_{\alpha}$ | 525 | 308 | 22 | 78 | 3 |
| | CuL $_{\alpha}$ | 930 | 713 | 15 | 85 | 4 |
| | MgK $_{\alpha}$ | 1254 | 1037 | 14 | 86 | 2 |
| 3s | CuL $_{\alpha}$ | 930 | 638 | < 10 | > 90 | • • • |
| | MgK $_{\alpha}$ | 1254 | 962 | 0 | 100 | 3 |



photoelectrons. Results of this paper agree satisfactorily with theoretical estimates.

ACKNOWLEDGMENTS

This work profited from fruitful cooperation with John W. Cooper and Steven T. Manson, both of the National Bureau of Standards, Gaithersburg, Maryland.

FIG. 4. Photolines (a) and angular distributions (b) of electrons ejected from 1s shell of neon. In this figure $\beta = v/c$.

* Research sponsored by the U. S. Atomic Energy Commission under contract with the Union Carbide Corporation.

¹H. Bethe, in *Handbuch der Physik* (Springer-Verlag, Berlin, 1933), Vol. 24.1; H. A. Bethe and E. E. Salpeter, in *Handbuch der Physik*, edited by S. Flügge (Springer-Verlag, Berlin, 1957), Vol. 35.

²A. P. Lukirskii, I. A. Brytov, and T. M. Zimkina, *Opt. i Spektroskopiya* **17**, 438 (1964) [English transl.:

Opt. Spectry (USSR) **17**, 234 (1964)].

³D. L. Ederer, *Phys. Rev. Letters* **13**, 760 (1964).

⁴J. A. R. Samson, *J. Opt. Soc. Am.* **53**, 507 (1963); *ibid.* **55**, 935 (1965).

⁵R. D. Deslattes, *Phys. Rev. Letters* **20**, 483 (1968).

⁶J. W. Cooper, *Phys. Rev.* **128**, 681 (1962); M. J. Seaton, *Proc. Phys. Soc. (London) Ser. A* **67**, 927 (1954); U. Fano, *Science* **153**, 522 (1966); J. W. Cooper, *Phys. Rev. Letters* **13**, 762 (1964).

⁷S. T. Manson and J. W. Cooper, *Phys. Rev.* **165**, 126 (1968).

⁸F. Combet Farnoux and Y. Heno, *Compt. Rend.* **264B**, 138 (1967); F. Combet Farnoux, *ibid.* **264B**, 1728 (1967).

⁹H. Hall, *Rev. Mod. Phys.* **8**, 358 (1936).

¹⁰M. O. Krause, T. A. Carlson, and R. D. Dismukes, *Phys. Rev.* **170**, 37 (1968).

¹¹T. A. Carlson, *Phys. Rev.* **156**, 142 (1967).

¹²J. W. Cooper and S. T. Manson, following paper, *Phys. Rev.* **177**, 157 (1969).

¹³W. Bothe, in *Handbuch der Physik* (Springer-Verlag, Berlin, 1933), Vol. 23.2, and references therein.

¹⁴J. Berkowitz and H. Ehrhardt, *Phys. Letters* **21**, 531 (1966); and J. Berkowitz, H. Ehrhardt, and T. Tekaat, *Z. Physik* **200**, 69 (1967).

¹⁵Z. Sujkowski, *Arkiv Fysik* **20**, 269 (1961).

¹⁶W. Bothe, *Z. Physik* **26**, 59 (1924); C. T. R. Wilson, *Proc. Roy. Soc. (London) Ser. A* **104**, 1 (1923); P. Auger, *Compt. Rend.* **188B**, 447 (1929).

¹⁷E. C. Watson and J. A. van der Akker, *Proc. Roy. Soc. (London) Ser. A* **126**, 138 (1930).

¹⁸M. O. Krause, *Phys. Rev.* **140**, A1845 (1965).

¹⁹M. O. Krause and T. A. Carlson, *Phys. Rev.* **149**, 52 (1966).

²⁰In Fig. 3a the continuum near the $KrM_{4,5}(MgK_{\alpha})$

line contains, however, a small contribution from $KrL_{2,3}-M_{4,5}$ Auger lines, and in Fig. 2 some weaker photolines interfere.

²¹For a review see U. Fano and J. W. Cooper, *Rev. Mod. Phys.* **40**, 441 (1968).

²²Charge spectra reported in Ref. 19 can readily be recalculated with the present experimental values for multiple-electron ionization and for the various subshell contributions.

²³F. W. Byron and C. J. Joachain, *Phys. Letters* **24A**, 616 (1967), and *Phys. Rev.* **164**, 1 (1967).

²⁴Some determinations of relative subshell cross sections by the same method have recently been reported by K. Siegbahn, C. Nordling, A. Fahlman, R. Nordberg, K. Hamrin, J. Hedman, G. Johansson, T. Bergmark, S. Karlsson, I. Lindgren, and B. Lindberg, *Nova Acta Reg. Soc. Sci. Upsaliensis Ser.* **20**, 1 (1967); J. A. R. Samson and R. B. Cairns [*Phys. Rev.* **173**, 80 (1968)] used a retarding-potential method to determine subshell contributions.

²⁵Preliminary data of the author on M and N subshell cross sections of Xe show satisfactory agreement with theoretical results of Ref. 7.

²⁶An attempt in this direction has been made by U. Fano and J. W. Cooper (see Ref. 21).

Photo-Ionization in the Soft X-Ray Range: Angular Distributions of Photoelectrons and Interpretation in Terms of Subshell Structure

John W. Cooper and Steven T. Manson*†

National Bureau of Standards, Washington, D. C. 20234

(Received 2 August 1968; revised manuscript received 25 October 1968)

The problem of determining the individual subshell contributions in atomic photoabsorption is discussed. The general form of the angular distribution of photoelectrons in the soft x-ray range for polarized and unpolarized incident photons is considered. Calculations of the subshell contributions within a central-field model and the angular distribution of electrons from these contributions for photoabsorption in Kr in the energy range 200–1500 eV are presented and found to show good agreement with the experimental results of the preceding paper.

I. INTRODUCTION

Absorption of radiation by atoms in the x-ray range is ordinarily considered as a two stage process. Radiation is absorbed and a single electron is emitted from one of the various subshells of the atom whose binding energy is less than the energy of the incident radiation. This initial photo-ionization process is followed by a rearrangement of the remaining electrons in the ionic core, accompanied by emission of fluorescent radiation or by secondary electrons. From this viewpoint absorption is considered as a single-electron process.

Direct measurements of the attenuation of radiation, while they provide absolute measurements of the absorption, provide no breakdown of the contributions of electrons from various subshells.

However, such a breakdown can be obtained from direct measurements of the energy distribution of electrons following absorption. While this technique is not new,¹ it has seldom been applied to determine a breakdown of subshell contributions to photoabsorption. Theory, on the other hand, determines uniquely the various subshell contributions to photoabsorption when subshell structure is explicitly represented by the wave functions describing the atomic system. Recent work^{2,3} has provided a breakdown into subshell contributions and has demonstrated that moderately good agreement with total absorption measurements may be obtained. However, the partitioning of the total absorption cross section into various subshell components has never been verified experimentally. The work described in the preceding paper⁴ rep-